GENERAL SYMPOSIA | INJECTION MOLDING

Investigations on Injection Mold Inserts with Reduced Thermal Masses using Additive Manufacturing

Milan Fitzlaff, Gibran Khoury, Moritz Käß, Martin Werz, Bernd Gundelsweiler and Stefan Weihe

DOI: https://doi.org/10.51573/Andes.PPS39.GS.IM.3

December 2024

Investigations on Injection Mold Inserts with Reduced Thermal Masses using Additive Manufacturing

Milan Fitzlaff, Gibran Khoury, Moritz Käß, Martin Werz, Bernd Gundelsweiler and Stefan Weihe[1]

Abstract: This work examined previously developed injection mold inserts with reduced thermal mass, with regard to lightweight construction approaches. These were optimised for oil-variothermal temperature control using simulative support. Additive manufacturing (AM), with its high degree of freedom in design, enables the implementation of individual, conformal cooling channels and can additionally support the efficiency of the variothermal process. The thermal mass of the injection mold is often a limiting factor in terms of process efficiency, which is also addressed in the analysis and optimisation considering the possibilities of additive manufacturing. A comparison of lightweight inserts with comparable variants made of solid material revealed a significant difference, with consideration of several tempering cycles. The validation of selected inserts confirmed the simulation. These investigations show that AM combined with lightweight construction approaches can support an additional increase in efficiency as well as a reduction in cycle times for the fluid-variothermal process control.

Keywords: Variotherm, Additive Manufactured Inserts, Injection Molding, Thermal Simulation

1 The authors Milan Fitzlaff (milan.fitzlaff@ikff.uni-stuttgart.de), Gibran Khoury and Bernd Gundelsweiler are affiliated with the Institute of Precision Engineering (IKFF) at the University of Stuttgart in Germany. Moritz Käß, Martin Werz and Stefan Weihe are affiliated with the Materials Testing Institute (MPA) at the University of Stuttgart in Germany.

DOI: https://doi.org/10.51573/Andes.PPS39.GS.IM.3

Introduction

Injection molding (IM) enables the economical mass-scale production of complex plastic components [1]. Variothermal temperature control is often required for parts with complex geometry or optical requirements. In this process, the mold is heated to a defined, required temperature prior to filling and cooled down afterwards for demolding [2]. In most cases, this is associated with an increase in cycle time. Faster and more efficient heating processes have therefore been the subject of several studies and can be achieved by various methods [3-6]. The least complex variant to implement regarding the mold design, and thus the dominating technology [6], is heating with fluids such as oil or water, since the same temperature control channels can be used for heating and cooling. A disadvantage is that the heat is generated outside the mold, which limits the dynamics of the process [7].

Due to the high degree of design freedom in the production of any component, additive manufacturing (AM) allows a decoupling of the design of cooling channels from the constraints of conventional manufacturing methods [8]. This enables a reduction of the thermal mass of the mold and is increasingly used for isothermal processes.

Fundamentals

Heat transfer must be differentiated into three mechanisms, all of which occur in IM: conduction, convection (also: convective heat transfer), and radiation [9]. The resulting heat flows based on these mechanisms, regarding the injection mold as a system boundary, is shown in Figure 1 [10].

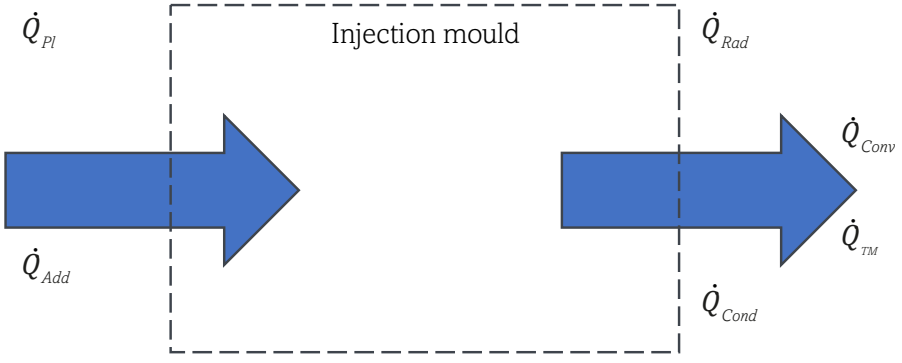

Figure 1. Heat flows at an injection mold (schematic).

The resulting total heat flow balance is given by equation 1 [11]:

DOI: https://doi.org/10.51573/Andes.PPS39.GS.IM.3

$$\dot{Q}_{Pl} - (\dot{Q}_{Cond} + \dot{Q}_{Conv} + \dot{Q}_{Rad}) + \dot{Q}_{Add} - \dot{Q}_{TM} = 0 \quad 1)$$

$\dot{Q}_{Pl}$ describes the heat flow coming into the system by the plastic melt. $\dot{Q}_{Cond}$, $\dot{Q}_{Conv}$ and $\dot{Q}_{Rad}$ are the heat losses due to conduction, convection, and radiation. $\dot{Q}_{Add}$ considers additional heat flows (e.g. using hot runner systems) and $\dot{Q}_{TM}$ gives the heat flow leaving the system with the cooling medium. The calculation of the heat flows is given in [9]. Another important factor is the thermal mass of a mold [7]. The heat Q supplied to or dissipated from a body with a mass m and a specific isobaric heat capacity c_p for a change in temperature ΔT is calculated using equation 2 [9]:

$$Q = c_p \cdot m \cdot \Delta T \quad 2)$$

Assuming Q and c_p are given and constant, the relationship given in equation 3 applies:

$$\frac{1}{m} \sim \Delta T \quad 3)$$

Accordingly, the smaller the mass of a body, the greater the change in temperature. This can also be achieved by thermally decoupling individual mold sections by means of insulating layers [7].

Scope of This Work

In this research, an oil-variothermal temperature control is optimized using AM. By combining the state-of-the-art and new developments, investigations are carried out for additive manufactured mold inserts. The aim of this work is to show suitable measures to make this process more efficient. As shown schematically in Figure 2, this on-going research project is divided into different phases. The overall development of the mold has already been subject in Fitzlaff et al. [12]. This research focuses on the third row of the process: thermal simulation and validation.

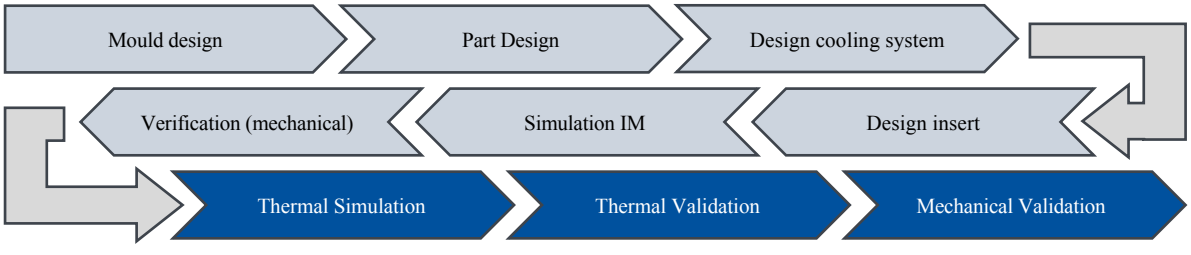

Figure 2. Schematic of the development process.

DOI: https://doi.org/10.51573/Andes.PPS39.GS.IM.3

Preparations and Implementation

Thermal Simulation

The inserts shown in Figure 3 are considered for thermal simulation. Insert V_{01} (a) consists of a component additive manufactured from stainless steel AISI 316L with conformal cooling channels to produce a cup-shaped part. This insert is back-casted with ultra-high performance concrete (UHPC) (in blueish grey). Due to its lower specific heat capacity and density [13], UHPC provides a lower thermal mass compared to the 316L. Furthermore, its lower thermal conductivity provides an additional insulation to the master mold. The V_{02} (b) insert made entirely of 316L bulk material serves as a reference in the simulation. In Fitzlaff et al. [12] a complex arcade like cooling system (ACS) with only 2 mm distance to the cavity surface has been developed. The V_{Gen} variant (c) uses the ACS in addition to an external lightweight structure for the production of a tensile test bar. Two additional reference inserts were modelled for this purpose. $V_{Gen,ref}$ (d) also uses the ACS, but does not have an external lightweight structure. $V_{Gen,ref-cc}$ (e) has an external lightweight structure and uses a conformal cooling system.

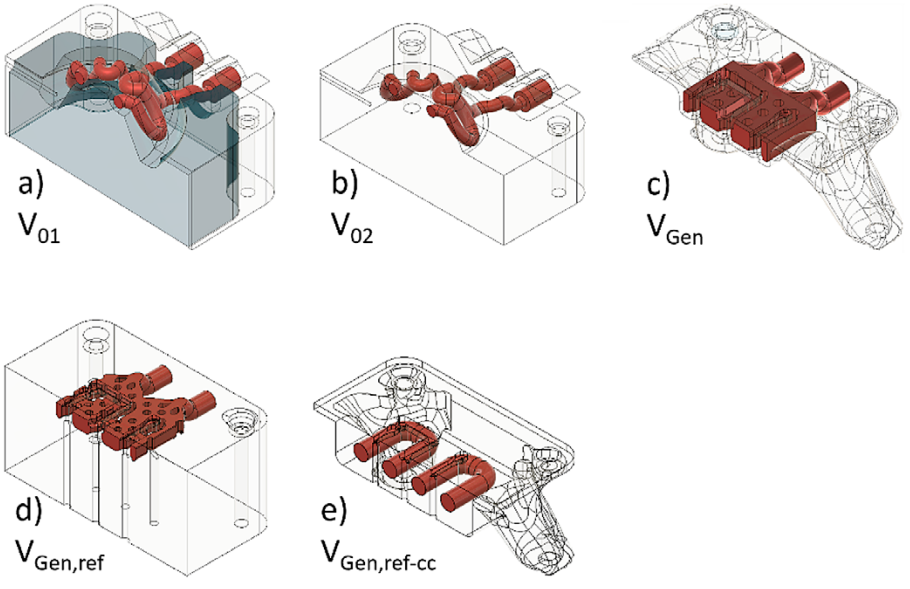

Figure 3. Designed inserts for the simulation (half section, cooling channel in red).

For the thermal simulation, a transient thermal simulation (ATTS) in "Ansys Workbench" (Ansys, Inc., Canonsburg, U.S.) in view of the similarity theory of heat transfer [9,14] is considered. The equations to determine the heat transfer coefficient α are given in [9]. Radiation was considered with an emission coefficient $\varepsilon = 0.36\ldots0.9$, [15]. Natural convection is included using the heat transfer coefficient $\alpha_n = 10\ \frac{W}{m^2 \cdot K}$ [14]. For the simulation, a mold target temperature $\vartheta_t = 125°C$ is

DOI: https://doi.org/10.51573/Andes.PPS39.GS.IM.3

defined for the process for V_{01} and V_{02}, using a fluid temperature ϑ_F = 145°C, limited in these investigations considering the properties of the UHPC used. For the inserts V_{Gen}, $V_{Gen,ref}$ and $V_{Gen,ref\ cc}$ a fluid temperature ϑ_F = 195°C is taken into account, for a mold target temperature of ϑ_t = 170°C. The target temperature already corresponds for V_{01} and V_{02} to the melt temperature of a polyethylene (PE)–Eraclene MS 80 U (Versalis S.p.A., Italy) [16], which was also used in the subsequent IM trials. The parameters of the simulation are summarized in Table 1.

Table 1. Parameters of the thermal simulation.

Variation	Fluid flow $\dot{V}\left[\frac{l}{min}\right]$	Fluid temp. $\vartheta_F[°C]$	Heat coefficient $\alpha\left[\frac{W}{m^2 \cdot K}\right]$
V_{01} and V_{02}	2x4.5	145–60	2359–860
V_{Gen} and $V_{Gen,ref}$	9	195–60	614 – 543
$V_{Gen,ref-cc}$	9	195–60	4318–1061

Thermal Validation

Thermal validation is carried out by taking thermographic images using a FLIR A655sc (Teledyne FLIR, Täby, Sweden) while the mold is open. The temperature is evaluated at ten points across the cavity, see Figure 4. The validation is performed on V_{01} and V_{Gen} with five repetitions each.

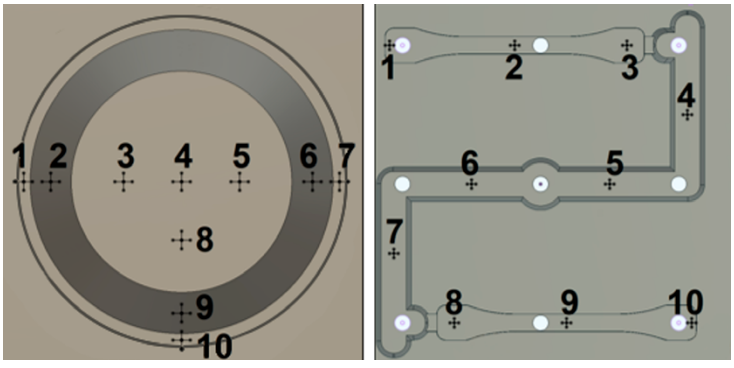

Figure 4. Measuring points for inserts V_{01} (left) and V_{Gen} (right).

Mechanical Validation

The investigations for mechanical validation are performed using the selected inserts on an injection molding machine, Arburg Allrounder 170S, (Arburg GmbH, Loßburg, Germany). The machine parameters are given in Table 2. Prior to the molding, as well as after 10 and 100 cycles, inserts V_{Gen} and V_{01} are inspected for visible damage by means of an optical inspection by the naked eye.

DOI: https://doi.org/10.51573/Andes.PPS39.GS.IM.3

In the same intervals, the inserts are inspected for deformations using a coordinate measuring machine “Prismo 7” (Zeiss GmbH, Oberkochen, Germany). Additional non-destructive examinations using a computer tomography (CT) “Phoenix V|tome|x M”, (Waygate Technologies, Huerth, Germany) enable an evaluation of the material condition inside the inserts and, thus, the detection of material failure.

Table 2. Parameters of the mechanical validation for selected inserts.

	V_{01}	V_{Gen}
clamping force [*kN*]	35	25
injection pressure [*MPa*]	20	16,5

Results and Discussion

Thermal Simulation and Validation

Figure 5(a) gives a comparison of the simulations and measurements for the inserts V_{01} and V_{02} for ϑ_F = 145°C and Figure 5 (b) for the inserts V_{Gen}, $V_{Gen,ref}$ and $V_{Gen,ref-cc}$ with ϑ_F = 195°C, showing the mean value of all points. The minimum and maximum temperatures are represented by error bars.

The measurements show a high consistency of the experiment with the simulation for cooling channels with a regular cross-section (V_{01}) for the considered inserts. The mold target temperature for V_{01} is reached at every point after only 22.2 s, which is consistent with the simulation (25.6 s). According to the simulation, a heating time of 90 s is to be expected for the insert V_{02}.

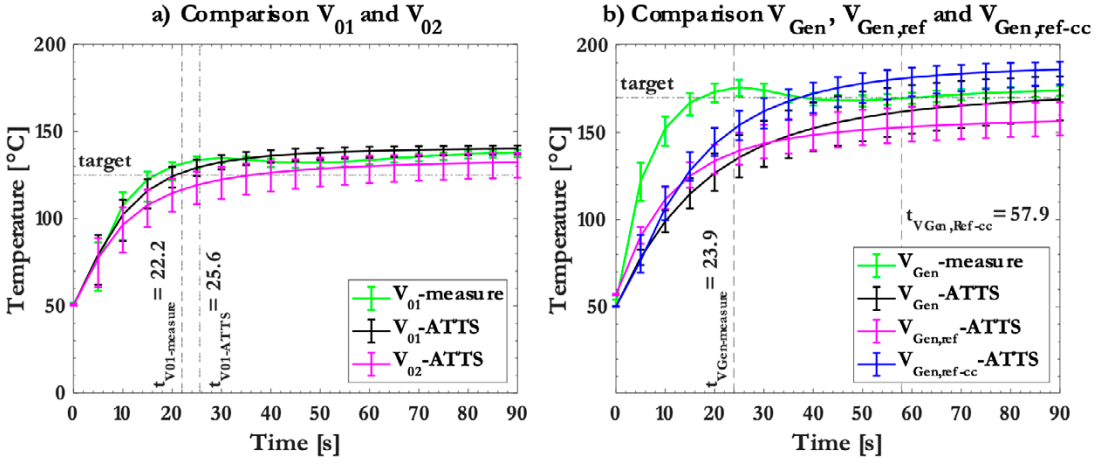

Figure 5. Comparison of V_{01} and V_{02} (a) and V_{Gen}, $V_{Gen,ref}$ and $V_{Gen,ref-cc}$ (b).

DOI: https://doi.org/10.51573/Andes.PPS39.GS.IM.3

For the insert with ACS (V_{Gen}), there is initially a higher deviation from the simulation and the mold target temperature is reached for the first time at every point after only 23.9 s. However, the temperature drops afterwards because remaining cold oil from the backflow of the mold is mixed with the oil from the hot circuit. As a result, the experiment and simulation are again consistent. This drop in temperature has been addressed in Regloplas AG [17] and can be counteracted with a suitable system. According to the simulation, the target mold temperature for the insert $V_{Gen,ref\text{-}cc}$ is reached after 57.9 s. Hence, with optimised peripheral equipment the ACS can outperform a conformal cooling system. Furthermore, the use of an ACS results in a more homogeneous surface temperature. It is also shown that the ATTS approach in the known method is only partially suitable for highly irregular cooling systems, such as the ACS.

These investigations suggest that a reduction of the thermal mass can reduce the required time to reach a target temperature in an oil-variothermal process by up to 50% to 66%.

Mechanical Validation

The measurements on the inserts on the coordinate measuring machine show no noticeable mechanical defects in the area around the cavity, even after 100 cycles. The CT results show no damage to the cooling systems. However, the visual inspection of insert V_{01} revealed the presence of microcracks and hairline fractures in the UHPC after ten cycles. The crack propagation progresses slightly after 100 cycles. Due to the high intensity of the x-ray beam, the CT is limited to further characterize the extent of these cracks. The hairline fractures in the concrete do not result in immediate failure of the mechanical stability of the insert. Endurance tests with periodic monitoring can provide a more precise prediction of the long-term stability of such an insert. Further methods for a reliable non-destructive testing must be evaluated.

Conclusion

The approaches used in this work show the possibility of reducing the cycle time for an oil-variothermal IM process and thus an improvement in efficiency. In simulation studies, the reduction of the thermal mass, the selection of materials with low thermal conductivity, and the reduction of contact surfaces between the insert and the master mold show a reduction in heat losses.

The simulative approach using the similarity theory of heat transfer is only of limited significance for complex cooling systems and therefore is initially less consistent. This discrepancy is compensated over time by a temperature drop in the system due to the cold oil in the return flow.

It has also been shown that the distance from the cooling system to the cavity can be reduced by using a complex, large-area cooling system, while still enabling a homogeneous temperature. This also has a positive effect on shortening the temperature control time. The use of thermally optimized

DOI: https://doi.org/10.51573/Andes.PPS39.GS.IM.3

inserts such as those developed in this research can therefore further increase the efficiency of a fluid-variothermal process and thus contribute to saving energy and cycle time.

References

1. C. Hopmann et al., *Spritzgießwerkzeuge: Auslegung, Bau, Anwendung,* 7th ed. München: Hanser; Ciando, 2018.
2. C. Bonten, *Kunststofftechnik: Einführung und Grundlagen,* 3rd ed. München: Hanser, 2020.
3. M. Deckert, "Beitrag zur Entwicklung eines hochdynamischen variothermen Temperiersystems für Spritzgießwerkzeuge," Dissertation, Technische Hochschule Chemnitz, Chemnitz, 2012.
4. S. Jacob, "Thermo-KonSens: Sachbericht (Schlussbericht) zum Verwendungsnachweis zu FuE Vorhaben," Leipzig, 2018.
5. M. Zülch, *Temperierung von Spritzgusswerkzeugen durch vollständig integrierte induktive Beheizung.* Dissertation. Stuttgart: IKFF, 2011.
6. W. Berlin et al., "Variothermie im Wandel der Zeit," *Kunststoffe*, vol. 109, no. 08, pp. 20-23, 2019.
7. C. Bleesen, "Variotherme Spritzgießtechnologie zur Beeinflussung tribologischer Eigenschaften thermoplastischer Formteile," Dissertation, TU Chemnitz, Chemnitz, 2016.
8. A. Kirchheim, "Additive Fertigung generiert Mehrwert," *Maschinenbau*, vol. 46, no. 8, pp. 32–33, 2018.
9. P. Stephan, S. Kabelac, M. Kind, D. Mewes, K. Schaber, and T. Wetzel, Eds., *VDI Wärmeatlas,* 12th ed. Berlin: Springer Vieweg, 2021.
10. G. Menges, G. Wübken, and B. Horn, "Einfluß der Verarbeitungsbedingungen auf die Kristallinität und Gefügestruktur teilkristalliner Spritzgußteile," *Colloid and Polymer Science*, vol. 254, no. 3, pp. 267–278, 1976.
11. M. Berghoff, "Perspektiven bei der Temperierung von Problemzonen im Werkzeug," Iserlohn, n. d.
12. M. Fitzlaff, G. Jäkle, and B. Gundelsweiler, "Additiv gefertigte Werkzeugeinsätze für den variothermen Spritzgießprozess," *Schriftenreihe / Institut für Kunststofftechnik, 28. Stuttgarter Kunststoffkolloquium: 28. Februar–2. März 2023*, C. Bonten and M. Kreutzbruck, Eds., Stuttgart: IKT Universität Stuttgart, 2023, pp. 259–266.
13. T. Litwin and B. Gundelsweiler, "Induktives Heißpressen von elektrisch leitfähigen Compound Werkstoffen," in *27. Stuttgarter Kunststoffkolloquium*, C. Bonten and Kreutzbruck Marc, Eds., 1st ed., Stuttgart, 2021, pp. 163–168.
14. H. Gröber and S. Erk, *Die Grundgesetze der Wärmeübertragung,* 3rd ed. Berlin: Springer, 1988.
15. KLEIBER Infrared GmbH, *Emissionsgradtabelle* Accessed: Nov. 6 2023. [Online]. Available: https://www.kleiberinfrared.com/index.php/de/amanwendungen/emissionsgrade.html
16. Versalis S.p.A, "Eraclene MS 80 U BCA: Technical Data Sheet," Milano, 2021.
17. Regloplas AG, *Einsparpotenzial bei der dynamischen Temperierung* Accessed: May 28 2024. [Online]. Available: https://www.regloplas.com/de/technologien/temperier-technologie/einsparpotenzial-bei-der-dynamischen-temperierung

DOI: https://doi.org/10.51573/Andes.PPS39.GS.IM.3